Lawrence Berkeley National Laboratory
LBL Publications

Title

Hierarchical electrode design of high-capacity alloy nanomaterials for lithium-ion batteries

Permalink

Journal

ISSN

Authors

Zhao, Hui
Yuan, Wen
Liu, Gao

Publication Date

DOI

Peer reviewed

Hierarchical electrode design of high-capacity alloy nanomaterials for lithium-ion batteries

Hui Zhao, Wen Yuan, and Gao Liu[*]

Environmental Energy Technologies Division,

Lawrence Berkeley National Laboratory, Berkeley, California 94720, USA

[*] Tel.: +1-510-486-7207; fax: +1-510-486-7303; Email: gliu@lbl.gov (G. Liu)

Summary: Nanomaterials and engineering approaches to assemble these nanomaterials play critical roles in the success of next-generation of high-energy-density electrochemical energy storage devices. As an on-going effort to increase the cycle life and energy densities of lithium-ion batteries, high-capacity alloy anodes, such as silicon, tin, and their alloys have attracted considerable attention due to their higher specific capacities (4200 mAh/g for Si, 994 mAh/g for Sn) compared to state-of-the-art graphite materials (372 mAh/g). These alloy materials are made into nano-size materials to achieve their full potential in capacity and life. The high-capacity material is assembled into a polymer laminate composite for a functional lithium-ion cell. However, these alloys experience a large volume change during lithiation and delithiation, and this disturbs the electrode integrity, causing its mechanical failure, including delamination from the current collector and cracking of the electrode. Unlike the traditional approach to electrode architecture, new materials and approaches have been developed to assemble nanoparticles into hierarchical structures to achieve high capacity and performance. In this hierarchical approach, polymer electrode binders are a critical component to address the large volume change induced by the high specific capacity during lithiation and delithiation. We summarize the recent explosive development of polymer electrode binders for alloy nanomaterials assembly, along with remaining challenges in this field.

Keywords: nanomaterials, nanomaterial assembly, polymer binder, silicon, solid electrolyte interphase, lithium-ion batteries, electrochemical energy storage

1. Introduction

Lithium-ion batteries (LIBs) have enabled the revolutionary development of cellphones and laptop computers, which has accelerated global communications.[1] In a charge process, lithium ions move from the electrolyte into the anode, and the electrons move from the external circuit through the current collector into the anode. Anode materials are reduced, and lithium ions intercalate into the graphene layers. To achieve this process, the anode laminate should be both electronic and ionic conductive. Electron transport is typically quite fast in the electrode materials (either cathode or anode), as is the ion transport in a typical liquid electrolyte, yet, the mobility of lithium ions inside the solid-state anode materials is a slow process. To overcome this issue of lithium ion transport in the solid-state anode material, a straightforward solution is to engineer the electrode materials into small-size particles to make a short ion transport path. The active electrode materials are produced as micron-size (graphite, $LiCoO_2$, $LiNi_{1/3}Mn_{1/3}Co_{1/3}O_2$) or nano-size (silicon, lithium iron phosphate) particles, depending on the ion mobility of different materials. On top of the ion mobility issue, most of the lithium-ion storage materials change volume during the lithium insertion and removal process, which creates internal stress, leading to material fracture when the material dimension gets larger. Therefore, mechanical integrity and good ionic and electronic conductivities are highly desirable in the design of an electrode laminate for LIBs. Polymeric binder is a critical component in the electrode, which adheres particles together and provides a cushion for the volume changes, an approach already widely used in the adhesive industry. A nano-size conductive additives (acetylene black) are added to provide electronic conductivity, enabling the electrode materials to access the electrons from the current collector. Both the porosity in the electrode and the swelling of the polymer binders by the electrolytes provide ionic conductivity. At the same time, the binders should not dissolve in the electrolyte, or they could disrupt the electrode architecture. The optimization of the electrode architecture[2,3,4] is important to achieve a satisfactory cell performance.

State-of-the-art LIBs widely use graphite as a negative electrode. Graphite is a crystalline, anisotropic carbonaceous material with stacked graphene layers, with ~0.335 nm distance between each layer. Graphite has a theoretical capacity of 372 mAh/g, and it undergoes a 10% volume change

during the process of lithiation and delithiation.[5] This process occurs below 0.25 V vs. Li, the voltage is sufficiently low to enable high-energy battery chemistry when coupled with a metal oxide cathode. As an on-going effort to search for the next-generation batteries with high capacity and long cycle life, alloy anodes made from materials such as Si and Sn have been drawing extensive attention due to their high storage capacities, which are 4200 mAh/g or 994 mAh/g for full lithiation to the $Li_{22}Si_5$ or $Li_{22}Sn_5$ phases, respectively. However, there have been no widespread applications of alloy anodes in Li-ion cells, mostly due to the large volume changes associated with Li-ion insertion and removal from the Si material.

Among various efforts to address the challenge, nanostructured active materials exhibit promising performance because of their ability to alleviate mechanical strain induced by volume change. It was shown that a critical diameter for fracture of Si nanopillars is between 240 and 360 nm during lithiation.[6] Smaller-size Si is less likely to undergo mechanical damage. Furthermore, a reduced diffusion path for lithium ions improves ionic conductivity.[7] The improved damage tolerance and lithium-ion conductivity enable better capacity retention for the Si nano-materials. Thus, the development of Si-based nano-materials has been a major focus in the effort of applying Si anode in LIBs.

Different forms of Si nano-structures, such as nanowires,[8,9] nanotubes,[10,11] and thin films[12] have been largely explored; yet, in the search for a commercial high-capacity anode material, the use of silicon nanoparticles is the most promising. The reason for this is two-fold: first, the commercial production of Si particles that could be used directly for LIB application has benefitted from their development in the semi-conductor industry; second, the form of the particles is compatible with state-of-the-art LIB industrial slurry preparation and the roll-to-roll lamination process.

However, simply using nanoparticles will not address all the problems. Active material pulverization can be largely avoided, but the drastic volume change of Si particles disrupts the integrity of the electrode and induces excessive side reactions, leading to fast capacity fade. Several mechanisms have been proposed to explain the capacity decay and cell failure,[13] including particle isolation from the binder/conductive additive network, electrode delamination from current collectors,

3

and continued solid electrolyte interphase (SEI)[14] growth. Mechanically, high-capacity electrode materials tend to generate more than an order of magnitude higher stress in the electrode than those of graphite during lithiation. The stress disrupts the mechanical integrity, leading to electrode fracture and delamination.[15]

More seriously, the electronic integrity of electrodes relies on the connections between the non-adhesive nano-size conductive additives and active materials. Even with extensive amount of conductive additive, this connection will break after extended cycles of large volume change particles.[16] The right polymer binder should provide good particle/particle cohesion to prevent particle isolation, and good laminate/current collector adhesion to prevent delamination. The intimate coating of polymer binder on the active material surface is able to modify the surface property during cell cycling; recent work also shows that the binder is involved in SEI formation and helps to stabilize the SEI during the drastic volume change.[17,18,19] An efficient battery binder is the ultimate solution for assembling high-capacity and high-volume-change electrodes. Nanostructured alloy anode materials for LIBs have been well-covered by several recent reviews.[13,20,21,22]

This review article focuses on the progress of assembly of high-capacity nanomaterials with polymer binders in LIBs. Although superior in many aspects to the micro- and bulk-size materials, nanomaterials have their own challenges of reduced density and large surface area, which make it difficult to maintain particle-to-particle connections for energy storage applications.
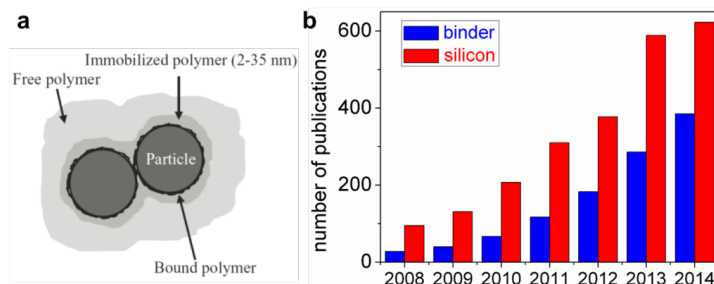

Figure 1. (a) The bulk polymer differentiates into three physical states when in contact with a particle surface. Bound polymer and immobilized polymer layers on a particle surface are defined as the fixed polymer layer. The free polymer forms a conduction path where electrons are carried from the current collector throughout the electrode laminate. Copyright 2012, The Electrochemical Society. (b) The number of peer-reviewed publications on the development of

4

binders or silicon anode for lithium-ion batteries as a function of the year published. Data were collected using the ISI Web of Science, with "binder" and "lithium ion battery" as search items in the "topic" box for the binder data, and "silicon" and "lithium ion battery" for the silicon data (search date: December 11th, 2014)

The exploration of assembly approach of nanomaterial with new polymers as binders for LIBs has rapidly advanced in recent years, as indicated by the large number of publications from 2008 to present day (Figure 1b). The corresponding data for silicon anode is shown for comparison. This trend obviously shows the global significance of polymer binders and the intensive interest of scientific research in this field. To deliver the highest power, the active materials in secondary batteries for portable electronics should fill out most of the restricted volume. Thus, the amount of any other electrode laminate compositions, such as binders, conductive additives, current collectors, and separators, should be reduced to a minimum, to reduce the polymer binder into just a nano-layer of coating on the Si particles. At the meantime, the demands for the lifetime and cycle numbers of the electrodes have dramatically increased for both electromobility and stationary applications.

From a theoretical point of view, polymer binders work similarly as polymer adhesives. An adhesive must satisfy two requirements to enable a good adhesion:[23]

(I)   The polymer must wet the surfaces, and spread to make a contact angle of close to zero;

(II)   After wetting, the polymer must harden to a cohesively strong solid. This process could be caused by a loss of solvent, chemical reaction, or cooling of the hot melt adhesives.

The slurry preparation should fulfill the first requirement, and loss of solvent by thermal drying is typically used to eliminate residual solvent and harden the polymer.

Several theories are used to explain the adhesion; the most common of which are physical adsorption and chemical bonding. Van der Waals forces across the interface are involved in the theory of physical adsorption, and the origin of the adsorption comes from permanent dipoles and induced dipoles. The use of polymer binders without any functional chemical groups such as polyvinylidene fluoride (PVDF) falls into this category. In contrast, other polymers, including poly(acrylic acid) (PAA), poly(vinyl alcohol) (PVA), and natural products with a high density of hydroxyl and carboxylic acid groups mainly use a chemical reaction (hydrogen bonding) to play the binder role.

Liu et al. introduced the physics of polymer composite to understand the LIB electrode structure

5

and performance. The surface area of the particles dominates the mixing process and polymer binder distribution. The polymer binder in the composite electrode will associate with the smaller-size conductive additive, even when the acetylene black (AB) is far from being the weight-dominant component of the electrode. The ratio of AB to binder is a critical parameter in optimizing electrode performance.[24,25] A high binder-to-AB ratio is beneficial because it creates a more cohesive conductive carbon particle network that results in better overall local electronic, and hence, reduced charge-transfer resistance. A similar conclusion was also made by Guyomard and coworkers.[26,27] Liu proposed a physical model in which polymer binder forms fixed nanometer-thick layers on the electrode active particle and AB surfaces (Figure 1a).[28] The extra free polymer provides a stronger binder force, but more of the free polymer binder tends to slow down ion transport at the interface. The active electrode (Si, Sn, or graphite) materials typically carry functional chemical groups from the production process;[29] the polymer binder tends to chemically bond or physically adsorb to the particle surface and form the fixed polymer layer. Addition of the AB conductive additives, which are nanoparticles with a large surface area, competes with the active material for the polymer binder and decreases the binding force in the electrode. The extra free polymer provides a stronger binder force, but more of the free polymer binder tend to slow down ion transport at the interface.
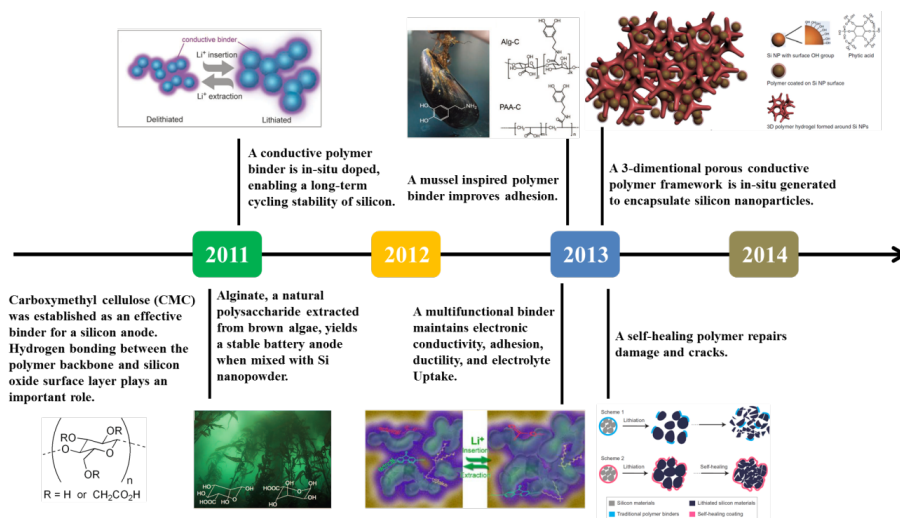

Figure 2. A brief timeline for the development of polymer binders for high-capacity alloy anodes.

The purpose of this review is to deliver an overview of the related progress in the assembly of nanomaterials with polymer binders in the application of high-capacity alloy-anodes in LIBs. Figure 2 shows the typical representative systems. Several categories of polymer binders in the literature, including conventional synthetic polymers, natural polymers and derivatives, conductive polymers, and other novel polymer systems are summarized. Equally important as new binder development, the recent advances in the characterization of polymer binder and electrodes are also discussed. The last section briefly summarizes this review and some key issues in this field.

2. Different types of binders developed for nano-Si and Sn anodes

2.1 Conventional synthetic polymer as binders

PVDF has been a standard polymer binder for graphite anodes and most of the metal oxide cathode materials. Lithium ions easily pass through a thin layer of swollen PVDF,[30] the lowest unoccupied molecular orbital (LUMO) of PVDF is high and it is expected that this polymer is stable in an anodic environment.[31]

Beaulieu et al. studied the effect of different binders for the high-capacity alloy anodes in LIBs. They realizied that the conventional PVDF binder only delivered poor cycling performance, and argued that the poor mechanical properties of PVDF could not tolerate the huge volumetric changes of the active material particles during charge/discharge cycles.[32] However, after a heat-treatment above the PVDF melting point, the binder could form a continuous film on the Si surface, which enabled a significantly better cycle life.[33] A fluorinated elastomer, poly(vinylidene fluoride-tetrafluoroethylene-propylene) (PVDF-TFE-P), was selected and its mechanical properties were comprehensively investigated.[34,35] The PVDF-TFE-P films could be extended to 100% strain either in air or ethylene carbonate (EC)/diethyl carbonate (DEC) solvents. The PVDF films, on the other hand, could not tolerate 10% elongation before break. The better mechanical properties of PVDF-TFE-P also translates into an improved battery cycling performance when used as a binder for an a-$Si_{0.64}Sn_{0.36}$ alloy anode.[36] In another work, Nafion, a sulfonated polymer with a polytetrafluoro-ethylene (PTFE) backbone, was used as binder for an Si anode.[37] The prepared electrodes showed a reversible specific

capacity of 800-1000 mAh/g when cycled between 0.9~0.17 V. A capacity retention of ~74% was reported after 100 cycles at a current rate of 150 mA/g.

PAA, and in some cases, its partially neutralized form, have been shown to be an effective binder for Si,[38,39] Si/graphite composite,[40,41,42,43] SiO,[44] and tin alloy[45] anodes. The effect of the neutralization on the binder performance is still controversial. It was shown that the viscosity of the PAA solution increases in the neutralized form.[46] A binder film with better ionic conductivity should be formed on the active material surface to facilitate the formation of more effective SEI and to enable better capacity retention and cycling performance. In another study, Wang and co-workers used PAA and PVA as a co-binder with a 9:1 ratio. The electrode laminate was heated at 150 ^{o}C for 1 hour to induce an esterification reaction to form a cross-linked gel polymer network.[47] An areal capacity of 4.3 mAh/cm^2 was achieved with Si nanoparticles, which is proposed to be due to the three-dimensional (3-D) interpenetrated network of the PAA-PVA binder. After five cycles the laminate based on PAA-PVA only shows a volume variation of 4.5%, this value is 19.7% for PVDF and 16.5% for CMC, which further confirmed the success of the cross-linked gel system.

2.2 Natural polymer and derivatives as binders for a nano-Si electrode

Before the advent of any synthetic polymers, nature had been using natural polymers as key components of any life form.[48] Polysaccharides, such as cellulose, alginate, and chitosan, prove to be effective polymer binders for high-capacity alloy-anodes in LIBs. The natural polymer binders rely on the functional groups, such as carboxylic acids and hydroxyl groups for adhesion. However, the downside is that there are different kinds of functional groups, and some may contribute to parasitic reactions and large irreversible capacities during cell cycling. Also, the natural products may have uncontrolled molecular weights, and the oligomer portion of the polymer will negatively influence the polymer's mechanical and binding properties. However, natural products are widely available and cheap, and the slurry preparation and lamination process are environmentally benign (in water). Both features make this family of binders promising candidates.

Three different polysaccharides (amylose, amylopectin, and glycogen) were examined as polymer binders for silicon/graphite composite electrodes.[49] Several different advantages were discovered

compared to PVDF: an improved first-cycle coulombic efficiency (CE) and suppressed electrolyte decomposition, and better cycling performance and capacity retention. Amylopectin exhibited the best electrochemical performance. One reason that the conventional PVDF binder does not work well for the Si anode is that the Si particles only attach to binders via weak van der Waals forces, and this binder fails to accommodate the drastic volume changes of Si particles during cycling. In another work, a natural polysaccharide binder, agarose, was used as a carbon source and polymer binder to increase the electrical conductivity of active materials.[50] The cross-linked binder was claimed to effectively cover macroporous Si particles, and a high reversible capacity (~2350 mAh/g) at a fast rate (10 Ah/g) was achieved with a CE of 89.8%.

Carboxymethyl cellulose (CMC), synthesized by a reaction between cellulose and chloroacetic acid, is a stiff polymer with a glass transition temperature of around 230 ^{o}C.[51] It was used as a thickener for a styrene-butadiene-rubber (SBR)/water dispersion-based slurry, since SBR only dispersed as small particles in water and the viscosity of the slurry needs to be improved by the dissolved CMC.[52] Liu et al. used SBR/CMC co-binder for a silicon-based anode, and a reversible capacity of 600 mAh/g for over 50 cycles was demonstrated.[53] Buqa et al. used SBR/CMC together as a binder for graphite/nano-silicon anode, and it showed an apparent advantage compared to PVDF. Buqa et al. revealed that the improvement actually came from CMC.[54] Li et al. clearly pointed out that the CMC binder was the origin of the advantageous performance in the above studies; they assembled electrode laminate using CMC and a commercial Si powder, which exhibited a specific capacity of 1100 mAh/g for 70 cycles, a vastly improved cycling performance compared to the PVDF-based Si laminate.[55]

Key et al. observed that after a full discharge of a lithium-silicon electrode, the open-circuit potential continued to increase even after 320 hours at room temperature, which they attributed to the reactivity of the metastable phase with the electrolyte and subsequent loss of lithium.[56] The CMC was shown to largely suppress this phenomenon, a relaxation of the open-circuit potential to 170 mV after a full lithiation took nine days in a binder-free system, while CMC delayed this period to a month. Taking advantage of the stiff nature of the CMC binder, Wang and co-workers used a slurry spray

9

technique to elaborate a CMC porous scaffold for Si anodes, and an improved cycling stability and rate performance was obtained.[57] Several research groups investigated the interaction between CMC and the surface active group on Si.[58,59,60] Guyomard and co-workers[61] showed that the extended conformation of CMC in solution facilitates a networking process of the conductive additive and Si particles during the composite electrode fabrication. By tuning the pH of the slurry, they were able to change the neutralization degree of the acid groups on CMC, and the favored interaction between Si and CMC could contribute to a remarkable cycle life of the nano-Si/CMC electrode.
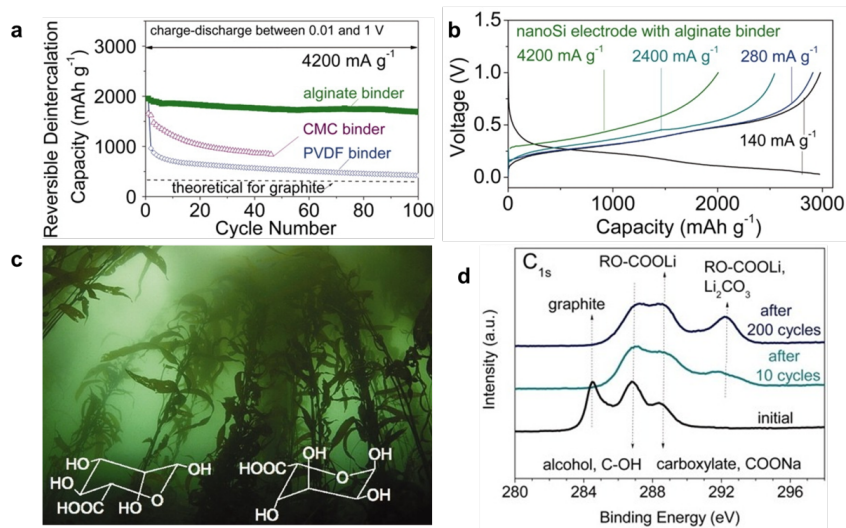
Figure 3. (a) Galvanostatic cycling performance of nano-Si electrodes with alginate, CMC, and PVDF binders at a current density of 4200 mA/g, in the voltage window of 0.01V-1V. (b) Charge/discharge voltage curves of the nano-Si electrode at different current densities. (c) Giant kelp forest (*Macrocystis pynfera* algae) in the Pacific Ocean, with the chemical structure of mannuronic (left) and guluronic (right) acids. (d) XPS C 1s spectra on the alginate-based Si anode before and after cycling. There are no major changes of the SEI chemistry after cycling for 10 or 200 cycles, indicating the stability of the SEI. Copyright 2011, The American Association for the Advancement of Science.

As mentioned in the section above, CMC was synthesized by functionalizing cellulose with chloroacetic acid. Since it is difficult to achieve a 100% conversion modification on a rigid polymer like CMC, it is not guaranteed that the carboxylic acid group is evenly present on every repeating unit. Alginate, a natural polysaccharide extracted from brown algae, is a copolymer of 1-4 linked β-D-mannuronic acid (M) and α-L-guluronic acid (G) residues (Figure 3c).[17] Carboxylic acid groups are

10

naturally present and averagely distributed in the polymer backbone. Electrode laminate based on Si nanoparticles and this natural binder exhibits a specific capacity of around 2000 mAh/g at a 1C rate (Figure 3a and 3b). Of a special notice is the effect of this binder on the SEI stability of the Si anode, as shown in the C 1s XPS data in Figure 3d. There is basically no obvious change of the SEI chemistry from 10th to 200th cycle, indicating good SEI stability. It is proposed that this excellent SEI stability provided by alginate is from the interaction between the electrolyte and the functional groups on alginate-a similar effect as in CMC/anode material systems.[62,59]

A carboxymethyl chitosan was explored as a water-soluble binder for a silicon/graphite composite electrode.[63] Fourier transform infrared spectroscopy (FTIR) spectra confirmed the bonding between the binder and the Si nanoparticle surface, and this new binder enabled better cycling performance of Si/graphite electrodes than CMC or alginate. Both CMC and PAA were used as co-binders and treated at a high temperature (150 $^{\circ}$C) to trigger esterification between the carboxylic acid groups on CMC and the hydroxyl groups on PAA.[64] A reversible capacity of over 2000 mAh/g after 100 cycles was obtained at room temperature, a superior capacity of 1500 mAh/g was achieved with a high current density of 7C (30 A/g) at 60 $^{\circ}$C. Elimination of the active groups and enhancing the mechanical property of the cross-linked bi-binder structure led to cell performance improvement.

The exceptional adhesion property of a mussel to adhere on a wet surface comes from a special structure moiety-catechol.[65,66] Ryou et al. incorporated catechol into alginate (Alg-C) and PAA (PAA-C), and the modified binder showed much improved binding and cycling performance compared to alginate and PAA.[67] The Alg-C-based Si electrode barely showed any capacity fade at a 3C rate compared to that at a C/10 rate. A specific capacity of around 2500 mAh/g-Si was obtained for both rates, with 3% fluoroethylene carbonate (FEC) additive in the electrolyte, at a loading of 0.2 ~ 0.3 mg/cm^2. Park et al. incorporated a photoreactive benzophenone group into PAA (PAA-BP) as a binder for Si-based anodes.[68] Nanoindentation and swelling measurements indicate enhanced mechanical properties of the photo-cross-linked PAA-BP binder, which limited the volume change marginally (38%) after full lithiation.

Jeong et al. treated β-cyclodextrin with epichlorohydrin under strong basic conditions to form a

hyperbranched *β*-cyclodextrin polymer (*β*-CDp).[69] Multidimensional hydrogen-bonding offers robust interaction with the Si particles; a self-healing effect was proposed which could recover the multidimensional binder network even if the Si nanoparticles were to lose their original contact with the binder during cycling. With a Si active material loading of 40 wt%, the lithium-ion half cell with *β*-CDp delivered a reversible capacity of around 1700 mAh/g at a 1C (4200 mA/g) rate, while alginate only exhibited a capacity of around 600 mAh/g.

2.3 Conductive polymer binders for nano-Si, Sn and sodium-ion battery

Conductive polymers are a category of functional polymers that have a delocalized π-system backbone. The highly conjugated backbone structure has reversible chemical, electrochemical, and physical properties controlled by a doping/de-doping process.[70] A novel concept was demonstrated that combined binding and conducting properties in the binder molecules (Figure 4), e.g., a conductive polymer binder.[71] Poly(9,9-dioctylfluorene-co-fluorenone-co-methylbenzoic ester) (PFM) has a polyfluorene-based structure, which is cathodically (reduction) doped in the Si electrode environment to achieve electrical conductivity. Adhesion groups (benzoate) are incorporated into the polymer binder to improve the integrity of the composite electrode. A PFM/nano-Si electrode without any conductive additives was fabricated. The electrode demonstrated over 650 cycles between 1 V and 0.01 V at the 2500 mAh/g-Si with only 20% capacity fade. The conductive polymer binders have opened a new paradigm of electrode design for Si materials, providing molecular-level electrical interaction between the electrode matrix and active materials and accommodating the volume expansion of high-capacity alloy materials.
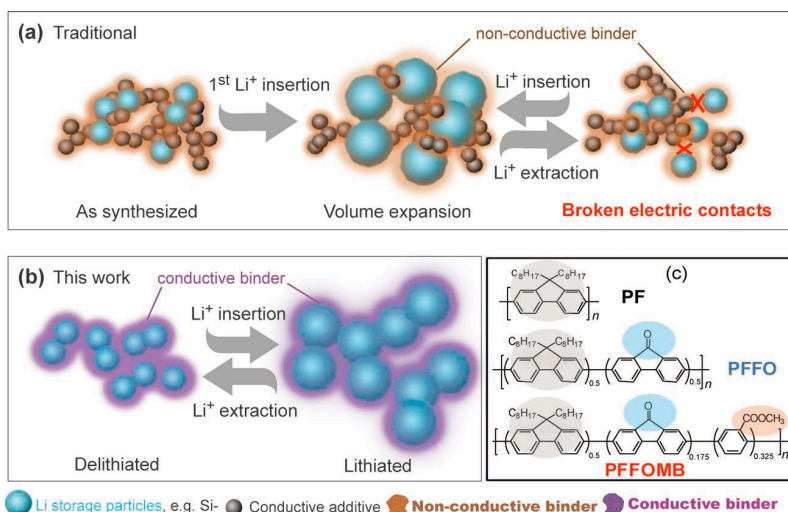
Figure 4. Schematics of the technical approaches to address the volume change issue in battery materials. (a) Traditional approaches use AB as conductive additive and PVDF polymer as the binder. (b) A conductive polymer with dual functionality, as a conductor and binder, could maintain the electrical and mechanical integrity of the electrode during the battery cycles. (c) The molecular structure of the PFM conductive polymer, with carbonyl and methyl benzoic ester, for tailoring the conduction band and for improving the mechanical binding force, respectively. Copyright 2011 Wiley-VCH.

As experimentally verified using synchrotron soft X-ray absorption spectroscopy (XAS) results and the density functional theory (DFT) calculations, the optimized electronic structure of PFM enables an in situ electron doping of the polymers under the Li-ion chemistry. The electronic conductivity of the PFM polymer reaches $4.9 * 10^{-6}$ S/cm after the first lithiation cycle. The conductivity is much lower than that of AB conductive additive particles because the doped electrons are somewhat localized as indicated by the isosurfaces.[71] The specific conductivity of AB is typically in the range from 0.1~100 S/cm, but both the particles and particle-to-particle connections for electron transport are rigid. The AB composite tends to lose electronic conductivity due to volume change of the Si materials. Therefore, such moderate improvement on conductivity of the conductive polymer binder over that of the nonconductive polymer binder has led to tremendous improvement of the Si electrode performance, as shown in Figure 4.
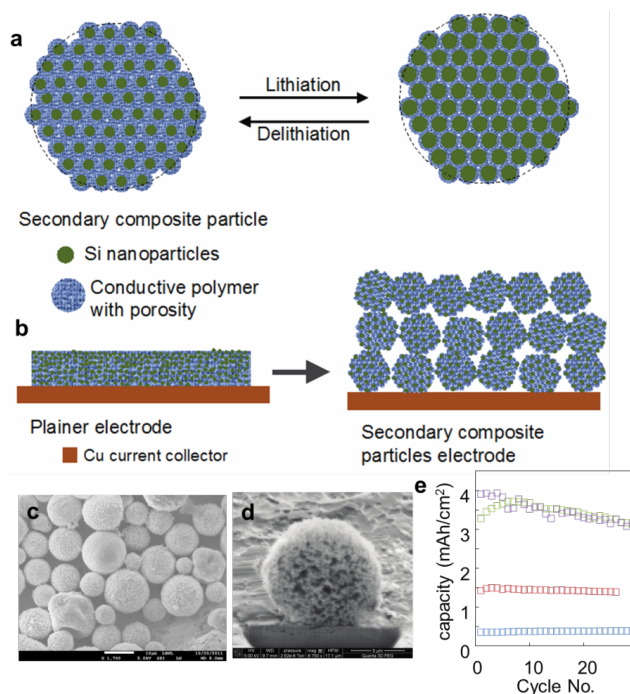
Figure 5. Schematic of the working principles of a hierarchal electrode design. (a) Secondary composite particles have a stable dimension during Si lithiation and delithiation. The dotted lines are for visual guidance. (b) A planar electrode made with a conductive polymer binder and Si nanoparticles vs. an electrode made with secondary composite particles. There are larger pores between the secondary composite particles. (c) Scanning electron microscope (SEM) images of the Si/conductive polymer secondary composite particles. (d) The cross-section morphology of a single secondary particle. (e) Cycling performance of the hierarchical electrode made with a Si/conductive polymer binder composite secondary particles, indicating a significantly improved loading and cycling stability. Copyright 2013, The Electrochemical Society.

Besides the electron transport issue, lithium-ion transport decay is another major issue within the Si-based electrode.[72] The mechanical movement of the electrode due to Si volume change during cycling alters the original structure of the Si electrode. Both experiments and modeling have confirmed that Si content needs to be below 40% (volUME, not considering porosity) in a composite electrode for a workable Si electrode.[73] In a conventional Si composite, the AB and binder tend to be pushed upward to the seal of the surface porosity and reduce the lithium-ion diffusion rate. Therefore, a thinner electrode performs much better than a thicker electrode, which decays very rapidly during cycling. This reduced lithium ion diffusion limits the critical dimension of the electrode thickness to

14

be around 10 µm based on our experiments of different thickness of the Si/PFM laminates. Si/PFM spherical particles with an average diameter of 10 µm were generated via a spray/precipitation method.[74] The hierarchical designed electrode with these secondary Si/PFM particles could achieve an areal capacity as high as 4 mAh/cm^2 with significantly better capacity retention and rate performance compared to the regular Si/PFM electrode system, as shown in Figure 5.
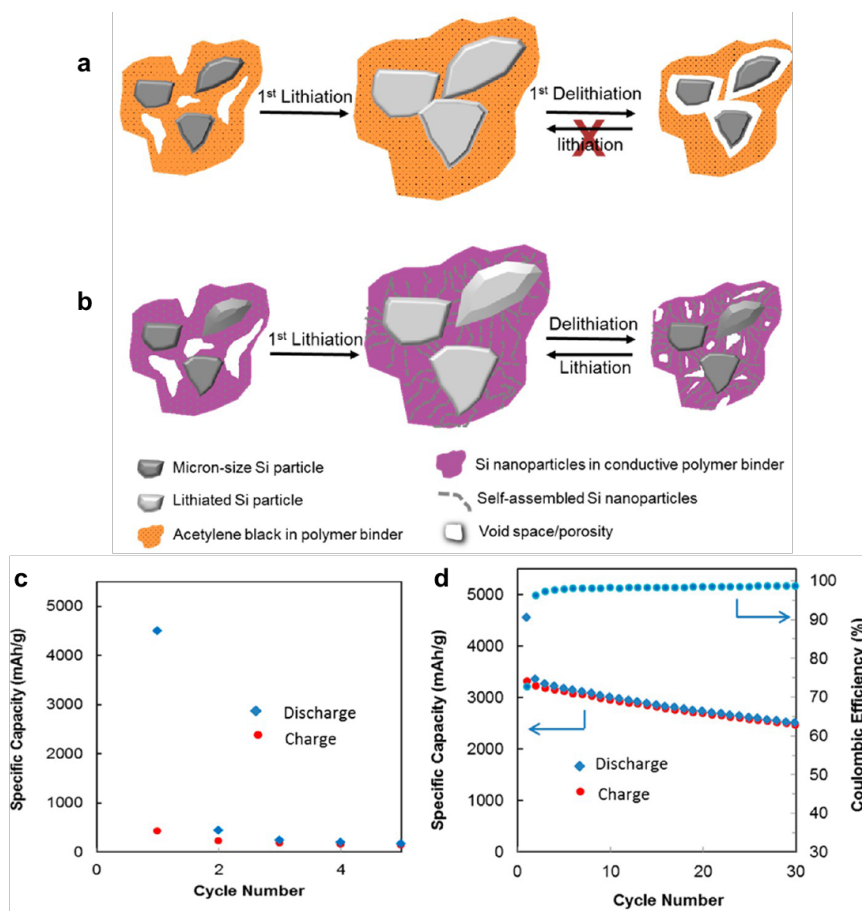

Figure 6. Schematics of the lithiation and delithiation process of composite anode electrodes using micrometer-size Si particles as active lithium-ion storage materials. (a) When AB is used, the absolute volume expansion of any individual particles is in the cube micrometer range. This large volume change has pushed the binders and AB composite to expand during the charge. During discharge, the AB/binder composite does not fully recover, leaving gaps between the Si active materials and the AB/binder conductive matrix. (b) When Si nanoparticles are used as an additive along with a conductive polymer binder during the charge process, the Si nanoparticles and micrometer-size Si tend to fuse to form a

network structure to cushion the volume expansion. The physical connections between the micrometer-size Si particles and the conductive network are preserved during the discharge process. Electrochemical performance of composite electrodes (c) m-Si/AB/PFM and (d) m-Si/n-Si/PFM. Copyright 2013, American Chemical Society.

To address the significant challenges associated with large volume change of micrometer-size Si (m-Si) particles as high-capacity anode materials for lithium-ion batteries, Si nanoparticles (n-Si) were used as a structural and conductive additive, with micrometer-size Si as the main lithium-ion storage material.[75] This system offers three advantages over conventional pure micrometer-size silicon-, AB-, and PVDF-based electrodes (Figure 6a and b): (1) The in-situ formed n-Si and m-Si 3D network takes advantage of the high surface area of small-size n-Si, thereby significantly alleviating the huge stress created by m-Si during the lithiation and delithiation process. (2) This network works like three-dimensional cross-linked advanced polymer binders, which have been shown in literature to help confine the Si particles in place, with higher resistance to strain—particularly nonrecoverable deformation. (3) A novel conductive polymer binder PFM can be used over the insulating PVDF to replace the nonbonding acetylene black. All three aspects play an indispensable role in this system's success. The resulting electrode showed a high specific capacity of 2500 mAh/g after 30 cycles with high initial coulombic efficiency (73%, Figure 6d) and good rate performance during electrochemical lithiation and delithiation: between 0.01 and 1 V vs Li/Li$^+$.

PFM has been successfully applied to other types of high-capacity anode materials for LIBs. Silicon oxide (SiO) has been considered to be a promising anode candidate for LIBs, with active Si dispersed in inactive silica as a nano-size domain. Two major obstacles have kept the SiO anode from reaching its full potential in LIBs: the excessive volume change of the micron-size SiO particles (compared to graphite), and the consumption of Li during the activation process (resulting in low first cycle coulombic efficiency). The PFM conductive polymer binder with a polar ester functional group is designed to adhere to the SiO$_2$ surface. Since the SiO$_2$ domains remain dimensionally stable in subsequent charge and discharge reactions, and are part of the stable surface of SiO materials, the adhesion between the functional conductive binder PFM and SiO materials is much more effective than in the Si system with the same functional conductive polymer binder (Figure 7a). PFM enabled

16

the reversible cycling of SiO above 1000 mAh/g for over 400 cycles at a C/10 rate in a half cell, with active SiO loading as high as 98 wt% (Figure 7b). XPS and TOF-SIMS analysis results indicate that the strong bonding between the silicon dioxide phase and functional conductive polymer binder results in good cycling performance with a minimum amount of binder.
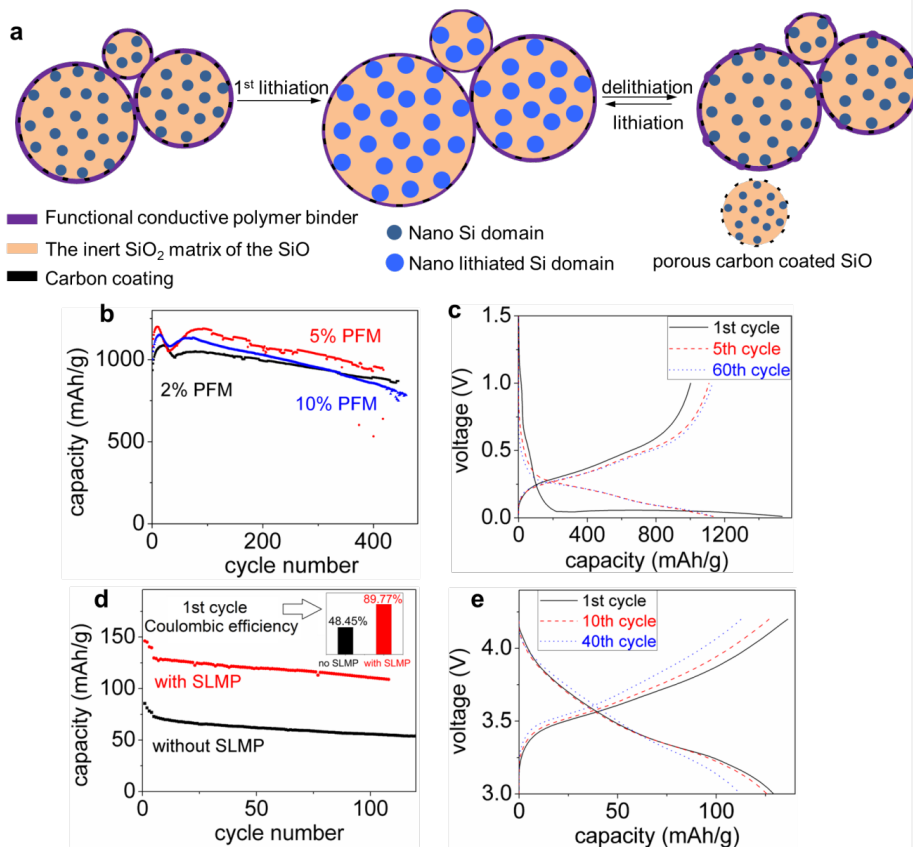

Figure 7. (a) The schematic of a low concentration of functional conductive polymer binder and SiO electrode. (b) Cycling performance in gravimetric capacity retention of SiO anodes with 2%, 5%, and 10% by weight of PFM binder using lithium counter electrodes at a C/10 rate (200 mA/g). (c) 1st, 5th and 60th cycle potential vs. capacity curves of a 2% PFM/SiO electrode. (d) SiO/NMC full cell performance with or without SLMP capacity enhancement additive, C/20 for 2 cycles, C/10 for 2 cycles and then C/3. (e) 1st, 10th and 40th cycle voltage curves of the SiO/NMC full cell with stabilized lithium metal powder (SLMP). Copyright 2014, American Chemical Society.

Another obstacle with the application of SiO materials in LIBs is that the first cycle CE of SiO is

low (50%~70%), so both SEI formation and interaction between lithium and silicon oxide (to form silicate) contribute to the large first-cycle irreversible capacity. This is a detrimental problem in a lithium-ion cell, since the lithium ion from the cathode will be irreversibly consumed. Stabilized lithium metal powder (SLMP®)[76,77] is used to prelithiate the SiO anode and compensate for the irreversible capacity loss in the first cycle. The first cycle CE in the SiO/NMC full cell was improved from 48% to ~90%, and an extraordinary capacity retention (>90% after 100 cycles at C/3) was realized by this unique strategy of using both functional conductive polymer binder and SLMP prelithiation (Figure 7d). PFM was shown to improve the cycling performance of a pure Sn nanoparticle at 520 mAh/g-Sn reversible capacity, with only 5% of the binder in the composite electrode.[78] Because of the high Sn loading in the laminate, the reversible capacity of the electrode could reach close to 500 mAh/g. The PFM/Sn anode is also successfully used in sodium ion battery, which delivers 806 mAh/g at C/50 and 610 mAh/g at C/10, exhibiting higher specific capacity and cycling stability compared with the Sn/CMC and Sn/PVDF electrode.[79]

As part of the on-going effort toward developing an ideal polymer binder design for high-capacity battery anodes, triethyleneoxide monomethylether (E in Figure 8) was incorporated into a conductive polymer to improve its polarity and enhance its electrolyte uptake capability. The challenge in designing a single-component battery binder is that modifications made to improve individual functionality must not be detrimental to one other; such impacts are circumvented by modifying only the side chains on the backbone of the polyfluorene conductive polymer.
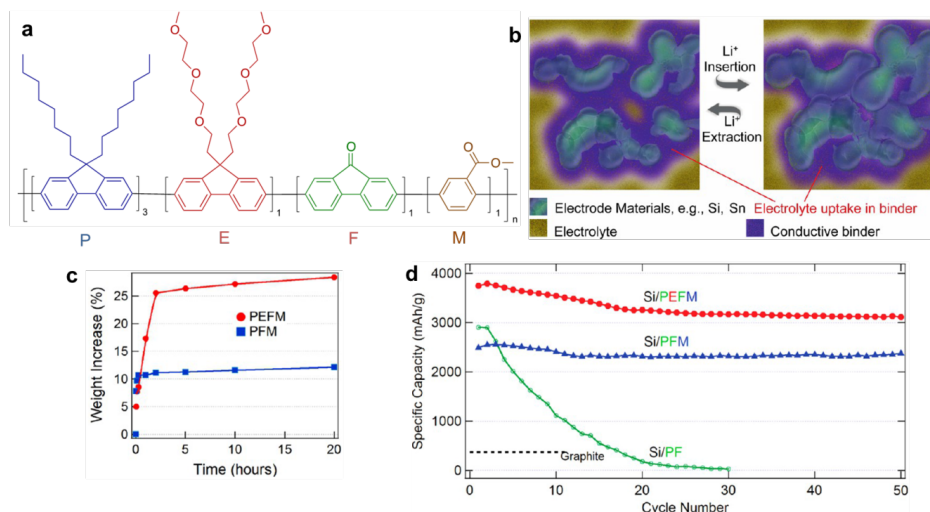
Figure 8. (a) Chemical structure of the PEFM binder. Functional groups contribute specific functionalities when the polymer is used as a binder in Li-ion batteries, P: polyfluorene with octyl side chains, contributes to the electronic conductivity, E: fluorenone with triethyleneoxide monomethyl ether side chains contributes to electrolyte uptake and mechanical property, F: fluorenone contributes to an optimized electronic conductivity, M: methyl benzoate ester contributes to good mechanical properties. (b) Schematic of an ideal binder system for high-capacity battery electrodes. (c) The swelling tests of PEFM and PFM polymer film in the 1 M LiPF$_6$ EC/DEC (1/1) electrolyte. The electrolyte uptake in PEFM is three times higher than that in PFM and is at the same level as that for a conventional PVDF binder. (d) Cycling performance of PFM/Si composite electrodes. PEFM enables the cycling with a full theoretical capacity of Si at 3750 mAh/g; the volume change of Si at this capacity is 100% higher than that of the PFM-based binder at 2500 mAh/g. Copyright 2013, American Chemical Society.

XAS and DFT calculation indicate that incorporation of E only leads to spectroscopic difference at higher energies away from the LUMO states, but has no effect on electronic conductivity.[80] The adhesion and swelling (electrolyte intake) have been the critical properties of the binder. The enhanced polarity of the PEFM polymer leads to a three-fold electrolyte uptake (Figure 8c). The PFM conductive binder has ~10% swelling in the standard EC/DEC (1/1 wt.) LiPF$_6$ electrolyte, while PEFM has 30% swelling.[53] A reversible capacity of 3500 mAh/g-Si was demonstrated with the modified binder (Figure 8d), which has close to 100% higher volume expansion than that in the PFM/Si system with a specific capacity at 2500 mAh/g, but the PEFM binder effectively maintained stable capacity over 50 cycles.
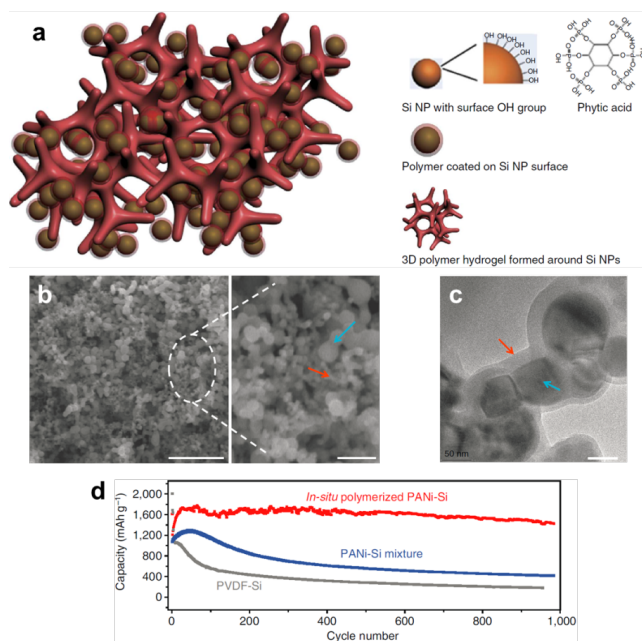
Figure 9. (a) Schematic description of the 3D porous Si nanoparticle/conductive polymer hydrogel composite electrodes. The silicon nanoparticles have been uniformly coated with a polymer layer. The interaction between Si nanoparticle and polymer is either between surface –OH groups and the phosphonic acids in the phytic acid crosslinker (right column), or the electrostatic interaction between negatively charged –OH groups and positively charged polyaniline due to phytic acid doping. (b) SEM image of a Si nanoparticle/polyaniline composite electrode at low (left) and high (right) magnifications. Scale bars are 1 μm (left) and 200 nm (right). (c) TEM image indicating the conformal coating of polyaniline layer on Si nanoparticles. (d) Galvanostatic cycling performance of the in situ polymerized Si nanoparticle/polyaniline composite electrodes with a current density of 1.0 A/g. The two control samples are Si nanoparticle/polyaniline without in situ polymerization and a Si nanoparticle/PVDF electrode. Copyright 2013, Macmillan Publishers Ltd.

Wu et al. introduced a conducting polymer hydrogel frame work for Si nanoparticles via in situ polymerization of aniline in the slurry preparation process. An aniline monomer was well-mixed with Si nanoparticles, and an oxidizer was then added to trigger the polymerization. The fabricated electrode laminate exhibited a reversible capacity of above 500 mAh/g at ~1.5 C for over 5000 cycles, with an areal capacity of ~0.7 mAh/cm.[2,18] Besides the conductive nature of this in situ formed polymer hydrogel, several other improvements contributed to the electrochemical stability of this Si composite electrode. First, the mixing process used low-viscosity aniline monomer, the following in

20

situ polymerization allows a conformal coating of the polymer onto Si nanoparticles; second, volume shrinkage was accompanied with this in situ process and the resulting porosity was supposed to help accommodate the volume expansion of Si particles; third, although pulverization of the large particles still occur during cell cycling, it is proposed that the conformal coating enabled good electrical connectivity among fractured particles (Figure 9a). An interesting observation was that the uniform conductive polymer coating enabled a deformable and stable SEI on the Si nanoparticles (Figure 9b and c). The positive results using in situ polymerization of conductive monomers have spurred follow-up work using other polymer structures such as pyrrole, combined with single-wall carbon nanotubes;[81] this design enabled a reversible delithiation capacity over 1600 mAh/g and 86% capacity retention after 1000 cycles at the current rate of 3.3 A/g, with an areal capacity of 0.4~0.7 mAh/cm^2 (Figure 9d). Kummer et al. assembled nano-Si/polyaniline (PAN) nanocomposites as anode material,[82] in which the nano-Si (with a mean crystallite size of 40 nm) was embedded into the PAN matrix.

Compared to the polyaniline and polypyrrole used in the previous work, poly(3,4-ethylenedioxythiophene) (PEDOT) has a higher electronic conductivity (10~1000 S/cm), which is a better choice for electrode applications.[83] A precursor water solution containing poly(3,4-ethylenedioxythiophene) doped with poly(4-styrenesulfonate) (PEDOT:PSS), super long (diameters of 30-80 nm and length of up to 1 mm) carbon nanotube (CNT), and silicon nanoparticles was gelated by addition of gelation agents (ammonium persulfate), which promoted the formation of a hydrogel Si electrode. Several advantages of this design were discussed: the long CNT could ensure the mechanical robustness and long-range conductivity of the composite electrode; PEDOT:PSS is a conductive polymer with decent electronic conductivity, and a four-point probe shows a conductivity of ~215 S/cm; and a PSS chain could cover the CNT surface, and the hydrophilic structure could interact with water, which facilitates the dispersion of CNT in water. A similar mechanism could also enable a good dispersion of the Si nanoparticles in the composite electrode. This combinatorial design enabled an impressive areal capacity of 2.2 mAh/cm^2 in the initial cycle and above 1.8 mAh/cm^2 after 100 cycles at a C/10 rate.

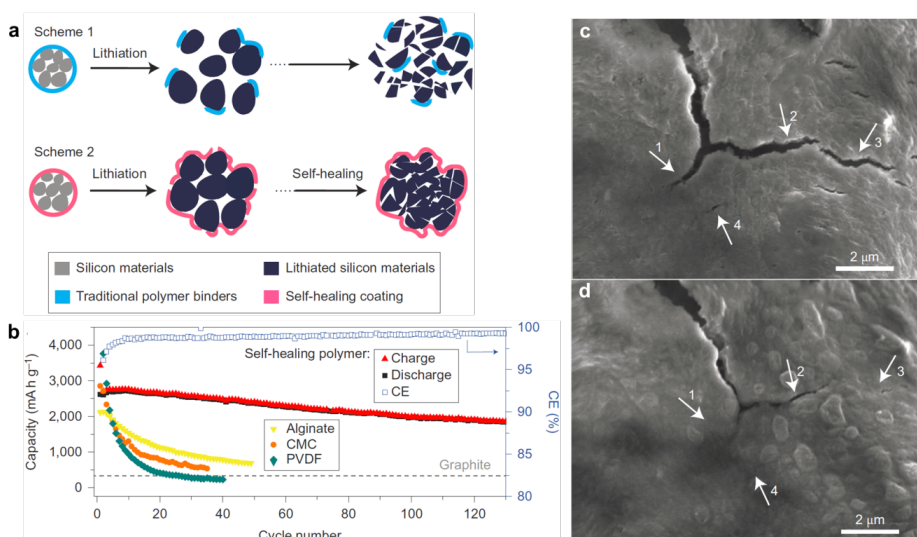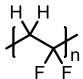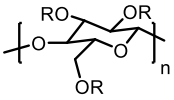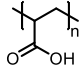**2.4 Other novel binders designed for a Si anode**

21
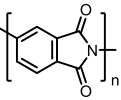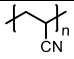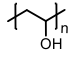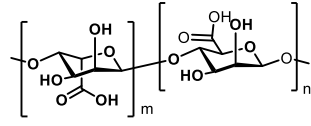
Figure 10. (a) Scheme 1: describes how particle cracking occurs using a conventional polymer binder, which leads to loss of electronic contact. Scheme 2: describes how the stretchable self-healing electrode maintains the electronic contact between cracked particles. (b) Galvanostatic cycling performance of Si microparticle electrodes with different polymer bi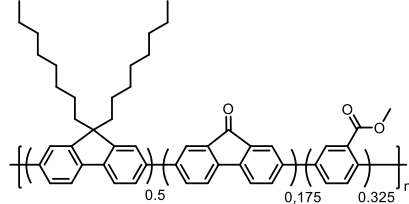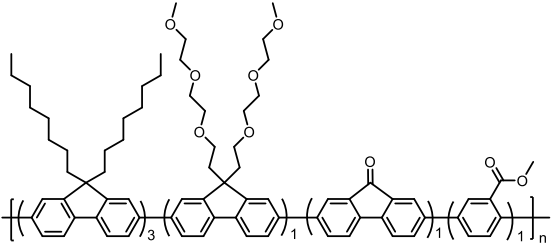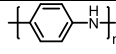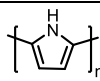nders, including the self-healing polymer and the conventional PVDF, CMC and alginate polymers. (c) Cracks in the polymer layer in the lithiated state. (d) Healed cracks after five hours, indicated by the arrows on the images. Copyright 2013, Macmillan Publishers Ltd.

All the binder designs summarized in the previous sections aim to avoid Si electrode failure during cell cycling, and most of the previous work utilized Si nanoparticles as active materials. However, the wide application of Si nanoparticles is limited since it is only available in small quantities. Silicon microparticles (SiMPs) serve as a promising alternative,[84] SiMPs are non-hazardous, cheap, and readily commercially available. Also the high tap-density of the micron-size particles facilitates the increase of the energy density of Si electrodes. However, compared to the nanoparticles, microparticles have even more serious structural changes, and the stress generated by the huge volumetric changes during the lithiation/delithiation of SiMPs induces fracture in the particles and polymer layers. This leads to the loss of electrical contact and causes extremely short cycling life over deep galvanostatic cycling.[85,57] Wang et al. synthesized a hydrogen-bonding-directed self-healing polymer via a step-growth polymerization between Empol 1016 (a mixture of diacids and triacids) and diethylenetriamine.[86,87] Both low T_g (~ 0 °C) and the hydrogen bonding in the polymer structure

contributed to a self-healing property. It is proposed that the self-healing nature of this material enables the healing of cracks and damage in the laminate coating during cycling (Figure 10a, c, d). The self-healing polymer binder enables the SiMPs (3~8 μm) to show a reversible capacity of 2600 mAh/g-Si at a C/10 rate for about 20 cycles. The mass loading of silicon was 0.5~0.7 mg/cm^2, leading to an areal capacity of 1.5~2.1 mAh/cm^2 (Figure 10b), an obvious increase of loading compared to many other previous reports using Si nanostructures.[88]

The performance of a lithium-ion cell relies on the concerted interaction of every single component in the cell, which includes active materials such as cathode and anode, as well as inactive materials such as binder, electrolyte, separator, etc. Table 1 lists comprehensive polymer structures that have been explored as binders for high-capacity alloy-anodes in the literature.

Polymer binders	Type of anode	Reference
 PVDF	Si, Sn, SiO, Si/C, Si-alloy	The use of PVDF binder was in lots of early work on Si or Sn anodes
 R = H or CH$_2$CO$_2$H CMC	Si, Sn, SiO, Si/C, Si-alloy	53, 54, 55, 58, 59
 PAA	Si, SiO, Si/C, Si-alloy	38, 39, 42,44,41,40
 Polyimide	SiO	89,90

Structure	Application	Ref.
 Polyacrylonitrile	Si/C	91
 Polyvinylalcohol	Si, Si/C	92,39
 Alginate	Si,	17
 Poly(9,9-dioctylfluorene-co-fluorenone-co-methylbenzoic ester) (PFM)	Si, Sn, SiO	71, 78,74,79
 Poly(2,7-9,9-dioctylfluorene-co-2,7-9,9-(di(oxy-2,5,8-trioxadecane))fluorene-co-2,7-fluorenone-co-2,5-1-methylbenzoate ester) (PEFM)	Si	80
 Polyaniline (PAN)	Si	87,82
 Polypyrrole (Ppy)	Si	81
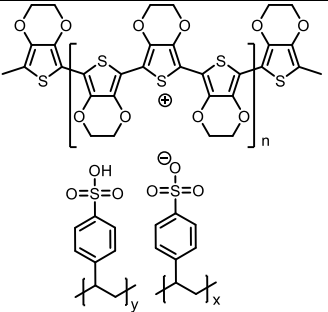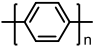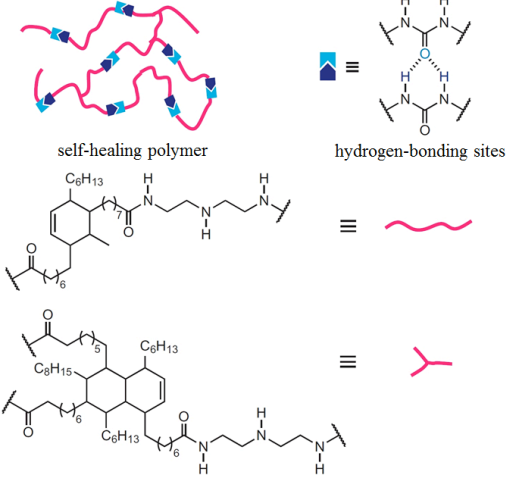
Structure	Anode	Ref.
 Poly(3,4-ethylenedioxythiophene) (PEDOT)	Si	83,93
 polyparaphenylene	Si	94
	Si	87

Table 1. A summary of the polymer binders developed for alloy anodes of LIBs.

3. Issues of concern

3.1 The influence of electrolytes

Although we cannot emphasize enough the importance of polymer binders in establishing stable cycling performance of high-capacity alloy anodes, the function of the polymer binder has to be considered in the whole lithium-ion cell, meaning that other aspects of the cell, such as the role of the

electrolytes, also must be taken into account.[95,96] Electrolyte additives were shown to be an effective and economic way of stabilizing SEI in LIBs.[97] Most of the work summarized in this review unanimously adopted FEC-containing electrolytes, varying from 2 wt% to 30 wt%. FEC is regarded as an effective electrolyte additive to form a stable SEI on Si or Sn anode. The exact role of FEC, as well as the structure of SEI formed by FEC, is a controversial and hot topic in the field.[98,99,100]

3.2 The influence of surface oxide layer on Si particles

A native oxide layer terminated with a hydroxyl group always exists in commercially available silicon materials. It is readily formed during synthesis, storage, and transportation due to the presence of trace amounts of oxygen and water. Most of the current studies on the Si anode employ Si nanomaterials, including spherical particles, wires, or sponge structures, which tend to have enhanced surface area compared to the conventional micron-size graphite particles.[39] Still under intensive investigation is to what extent or under what conditions the SiOx species can be electrochemically reduced by lithium. Most of the reports show that the reduction products of this SiOx layer include Li_2O,[101,102] and different forms of silicates such as Li_4SiO_4,[101,103,104,105,106] $Li_2Si_2O_5$,[104,105] Li_2SiO_3,[106] etc. This surface SiO_2 layer was shown to contribute to a higher first-cycle capacity loss compared to that of the Si samples etched by hydrofluoric acid.[107,29] However, from the binder point of view, existing functional groups on the Si surface provide a reaction point with the polymer binders. This has been regarded as the origin of some useful binders, such as PAA, CMC, and alginate, for Si-based anodes.

3.3 Characterization of the mechanical property of binders and electrodes

The criteria of a good binder for a high-capacity alloy-anode lie on the improvement of electrochemical performance, i.e., cycling stability and CE. A good adhesion property, including particle/particle cohesion and laminate/Cu adhesion, also is an important prerequisite for a good binder. The mechanical property of a binder also affects the battery manufacturing; cell manufacturing processes such as winding and calendering could potentially unbind particles and/or lead to electrode delamination from the current collector. A delaminated electrode results in the loss of active materials; detached particles such as active material particles and a conductive additive may penetrate the

26

separator during winding and cause the cell to short.[108]

A peel test is normally used to analyze the adhesion strength provided by polymer binders in LIB electrodes.[80,16,109,110] For this test, adhesive tape is stuck onto the surface of an electrode. A high-precision micromechanical test system measures the peel strength while pulling the adhesive tape off the electrode. However, this method is highly dependent on the test conditions, such as the initial adhesion between the tape and the electrode surface, the type of the adhesive tapes, etc. In addition, the peel test results only reflect the adhesion property between the tape and the electrode surface, rather than the cohesion between particle/particle and adhesion between the electrode laminate and the current collector. Thus, to understand the mechanical property of the binder and electrode from a fundamental point of view, some other characterization techniques were developed.
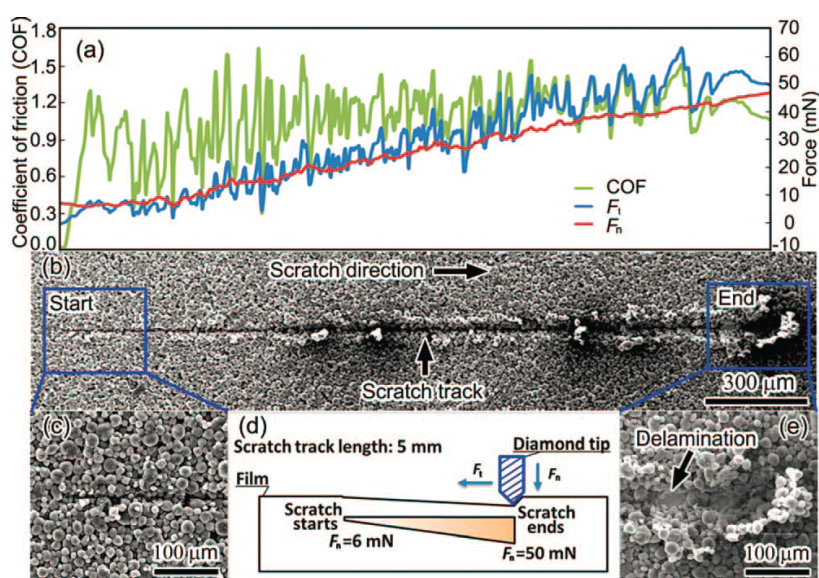
Figure 11. (a) Normal force F_n, tangential force F_t, and coefficient of friction curve of a MCMB/PVDF composite electrode as a function of scratching distance. (b) SEM image of the scratch track. (c) and (e) SEM images of the beginning and the end of the scratch track. (d) Schematic description of the scratch test. Copyright 2013, The Electrochemical Society.

A microscratch test was developed[111] employing a conical diamond stylus with a tip radius of 1.5 μm and a cone angle of 60°. The scratch tip approached the film surface, and a 2 mm long scratch

track was made by translating the sample while linearly ramping up the normal load on the conical tip. The tangential force F_n and normal force F_t were measured in real time (Figure 11a). The particle/particle cohesion strength was semi-qualitatively evaluated by analyzing the coefficient of friction (COF), which can be readily calculated by F_n/F_t. Figure 11 shows the schematic illustration of the scratch test, as well as the scratch tack and measured tangential and normal forces.

4. Concluding remarks and outlook

Recent work on the binder development establishes the binder as a key component to enable the application of high-capacity alloy-anodes, such as silicon and tin in LIBs. Take silicon as an example: specific capacities of 2000 mAh/g at low rate (0.1C) or 1500 mAh/g at a high rate (0.5C~1C) for long-term cycling (over 500 cycles) are now well achieved. Still many issues remain to be solved before producing a commercial application of alloy anodes:

1. Most of the work on silicon anodes, including the development of new binders and modification of silicon active material, focuses on high value and stable specific capacity. However, as shown by Dahn et al.,[112] specific capacity may not be so indicative of the ultimate performance of an electrode's active materials. The loading of the silicon per area is still quite small in most of the current work, with an areal capacity of typically less than 0.5 mAh/cm^2. This does not gain much advantage compared to the state-of-the-art graphite anodes, which could easily attain an areal capacity of ~3 mAh/cm^2. Several recent publications show that scientists in this field already are devising different solutions for this problem,[74,113] so it is expected that more attention will be drawn toward a high-loading silicon electrode.

2. The conventional PVDF binder works well for different types of graphite anodes and cathode material; however, this is not the case for the alloy-anodes. Alloy-anode materials generated from different production processes, varying at different particle sizes, tap densities, surface chemistries, and specific capacities (volume changes) typically prefer a specific binder over another. This explains some of the data discrepancy from different research groups. For example, in one publication, alginate enables the best performance of a Si anode,[17] while

28

another work, although employing the same electrode composition and testing procedure, shows that PAA gives the best performance.[39] The former work used Si nanoparticles from MTI Corporation, and the latter obtained its Si from Alfa Aesar. The different sources of Si active materials might explain the different performances using different binders. This "specific binder for a specific active material" rule indicates our paucity of understanding on the role of binders for alloy anodes in LIBs. Although many important pieces of the jigsaw puzzle that enlightens us about the interaction of polymer binders and anode active particles have been discovered, they do not quite connect.

3. Most of the work on binders for Si anodes, or even the research on alloy-anodes as a whole, focuses on the half-cell study with lithium metal as a counter electrode. The use of the Si anode has to be considered in a real lithium-ion full cell. Several questions need to be answered: if a stable cycling performance could be achieved in a lithium-ion full battery, is there any gain on energy density by incorporating Si into LIBs? Should we use pure Si or Sn as anodes, or would it be better choice to use a mixture of graphite/alloy anodes? Some of the recent work shows that people are already seriously considering these questions. Obrovac and co-workers investigated the effect of calendering and mixing graphite to composite electrodes comprising Si alloy particles.[114] Their systematic study indicates that only when alloys are blended with graphite and calendered to high densities, can the best cycle life, the highest energy density, and the lowest volume expansion electrodes be obtained. It is believed that this is the most likely way the high-capacity alloys could be utilized in commercial cells.

Regardless of the existing challenges, significant progress has been made on the development of polymer binders as a key electrode component to enable the application of high-capacity alloy anodes for a hierarchical electrode design of Si and Sn nanomaterials for LIBs.

<div style="text-align:center">
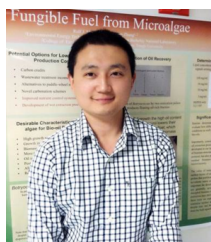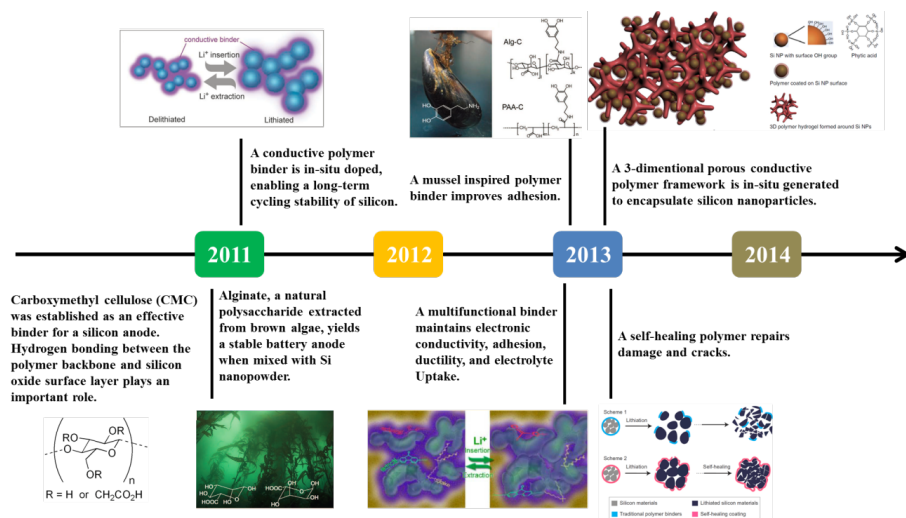
Acknowledgements

</div>

References

1. J. B. Goodenough and K.-S. Park, *J. Am. Chem. Soc.*, 2013, **135**, 1167-1176.
2. M. Ebner, F. Geldmacher, F. Marone, M. Stampanoni and V. Wood, *Advanced Energy Materials*, 2013, **3**, 845-850.
3. M. Ebner, F. Marone, M. Stampanoni and V. Wood, *Science*, 2013, **342**, 716-720.
4. M. Ebner, D.-W. Chung, R. E. García and V. Wood, *Advanced Energy Materials*, 2014, **4**, n/a-n/a.
5. R. Fong, U. von Sacken and J. R. Dahn, *J. Electrochem. Soc.*, 1990, **137**, 2009-2013.
6. S. W. Lee, M. T. McDowell, L. A. Berla, W. D. Nix and Y. Cui, *Proceedings of the National Academy of Sciences*, 2012, **109**, 4080-4085.
7. P. G. Bruce, B. Scrosati and J.-M. Tarascon, *Angewandte Chemie International Edition*, 2008, **47**, 2930-2946.
8. C. K. Chan, H. Peng, G. Liu, K. McIlwrath, X. F. Zhang, R. A. Huggins and Y. Cui, *Nat Nano*, 2008, **3**, 31-35.
9. R. Deshpande, Y.-T. Cheng and M. W. Verbrugge, *Journal of Power Sources*, 2010, **195**, 5081-5088.
10. M.-H. Park, M. G. Kim, J. Joo, K. Kim, J. Kim, S. Ahn, Y. Cui and J. Cho, *Nano Letters*, 2009, **9**, 3844-3847.
11. J.-K. Yoo, J. Kim, Y. S. Jung and K. Kang, *Advanced Materials*, 2012, **24**, 5452-5456.
12. Y. He, X. Yu, Y. Wang, H. Li and X. Huang, *Advanced Materials*, 2011, **23**, 4938-4941.
13. H. Wu and Y. Cui, *Nano Today*, 2012, **7**, 414-429.
14. F. Shi, H. Zhao, G. Liu, P. N. Ross, G. A. Somorjai and K. Komvopoulos, *The Journal of Physical Chemistry C*, 2014.
15. J. H. Ryu, J. W. Kim, Y.-E. Sung and S. M. Oh, *Electrochemical and Solid-State Letters*, 2004, **7**, A306-A309.
16. C.-M. Park, J.-H. Kim, H. Kim and H.-J. Sohn, *Chemical Society Reviews*, 2010, **39**, 3115-3141.
17. I. Kovalenko, B. Zdyrko, A. Magasinski, B. Hertzberg, Z. Milicev, R. Burtovyy, I. Luzinov and G. Yushin, *Science*, 2011, **334**, 75-79.
18. H. Wu, G. Yu, L. Pan, N. Liu, M. T. McDowell, Z. Bao and Y. Cui, *Nature Communications*, 2013, **4**, 6.
19. S.-J. Park, H. Zhao, G. Ai, C. Wang, X. Song, N. Yuca, V. S. Battaglia, W. Yang and G. Liu, *Nature Communications*, 2014, **5**, Accepted.
20. X. Su, Q. Wu, J. Li, X. Xiao, A. Lott, W. Lu, B. W. Sheldon and J. Wu, *Advanced Energy Materials*, 2013, **4**, 1300882.
21. K.-Q. Peng, X. Wang, L. Li, Y. Hu and S.-T. Lee, *Nano Today*, 2013, **8**, 75-97.
22. Y. Xu, Q. Liu, Y. Zhu, Y. Liu, A. Langrock, M. R. Zachariah and C. Wang, *Nano Letters*, 2013, **13**, 470-474.
23. J. Comyn, *Adhesion Science*, The Royal Society of Chemistry, Thomas Graham House, Science Park, Milton Road, Cambridge CB4 4WF, UK 1997.
24. G. Liu, H. Zheng, A. S. Simens, A. M. Minor, X. Song and V. S. Battaglia, *Journal of The Electrochemical Society*, 2007, **154**, A1129-A1134.
25. G. Liu, H. Zheng, S. Kim, Y. Deng, A. M. Minor, X. Song and V. S. Battaglia, *Journal of The Electrochemical Society*, 2008, **155**, A887-A892.
26. D. Guy, B. Lestriez, R. Bouchet, V. Gaudefroy and D. Guyomard, *Electrochemical and Solid-State Letters*, 2005, **8**, A17-A21.
27. D. Guy, B. Lestriez, R. Bouchet and D. Guyomard, *J. Electrochem. Soc.*, 2006, **153**, A679-A688.
28. G. Liu, H. Zheng, X. Song and V. S. Battaglia, *Journal of The Electrochemical Society*, 2012, **159**, A214-A221.
29. S. Xun, X. Song, L. Wang, M. E. Grass, Z. Liu, V. S. Battaglia and G. Liu, *Journal of The Electrochemical Society*, 2011, **158**, A1260-A1266.
30. E. Tsuchida, H. Ohno and K. Tsunemi, *Electrochim. Acta*, 1983, **28**, 591-595.
31. A. Kurihara and A. Nagai, in *The 39th Battery Symposium in Japan*, 1998, p. 309.
32. L. Y. Beaulieu, K. W. Eberman, R. L. Turner, L. J. Krause and J. R. Dahn, *Electrochemical and*

Solid-State Letters, 2001, **4**, A137-A140.

33. J. Li, L. Christensen, M. N. Obrovac, K. C. Hewitt and J. R. Dahn, *Journal of The Electrochemical Society*, 2008, **155**, A234-A238.

34. Z. Chen, L. Christensen and J. R. Dahn, *Journal of Applied Polymer Science*, 2003, **90**, 1891-1899.

35. Z. Chen, L. Christensen and J. R. Dahn, *Journal of The Electrochemical Society*, 2003, **150**, A1073-A1078.

36. Z. Chen, L. Christensen and J. R. Dahn, *Journal of Applied Polymer Science*, 2004, **91**, 2958-2965.

37. R. R. Garsuch, D.-B. Le, A. Garsuch, J. Li, S. Wang, A. Farooq and J. R. Dahn, *Journal of The Electrochemical Society*, 2008, **155**, A721-A724.

38. A. Magasinski, B. Zdyrko, I. Kovalenko, B. Hertzberg, R. Burtovyy, C. F. Huebner, T. F. Fuller, I. Luzinov and G. Yushin, *ACS Applied Materials & Interfaces*, 2010, **2**, 3004-3010.

39. C. Erk, T. Brezesinski, H. Sommer, R. Schneider and J. Janek, *ACS Applied Materials & Interfaces*, 2013, **5**, 7299-7307.

40. N. Yabuuchi, K. Shimomura, Y. Shimbe, T. Ozeki, J.-Y. Son, H. Oji, Y. Katayama, T. Miura and S. Komaba, *Advanced Energy Materials*, 2011, **1**, 759-765.

41. S. Komaba, N. Yabuuchi, T. Ozeki, Z.-J. Han, K. Shimomura, H. Yui, Y. Katayama and T. Miura, *The Journal of Physical Chemistry C*, 2011, **116**, 1380-1389.

42. Z.-J. Han, N. Yabuuchi, K. Shimomura, M. Murase, H. Yui and S. Komaba, *Energy & Environmental Science*, 2012, **5**, 9014-9020.

43. Z.-J. Han, N. Yabuuchi, S. Hashimoto, T. Sasaki and S. Komaba, *ECS Electrochemistry Letters*, 2013, **2**, A17-A20.

44. S. Komaba, K. Shimomura, N. Yabuuchi, T. Ozeki, H. Yui and K. Konno, *The Journal of Physical Chemistry C*, 2011, **115**, 13487-13495.

45. J. Li, D.-B. Le, P. P. Ferguson and J. R. Dahn, *Electrochimica Acta*, 2010, **55**, 2991-2995.

46. M. Masiak, W. Hyk, Z. Stojek and M. Ciszkowska, *The Journal of Physical Chemistry B*, 2007, **111**, 11194-11200.

47. J. Song, M. Zhou, R. Yi, T. Xu, M. L. Gordin, D. Tang, Z. Yu, M. Regula and D. Wang, *Advanced Functional Materials*, 2014, n/a-n/a.

48. M. Ling, J. Qiu, S. Li, H. Zhao, G. Liu and S. Zhang, *Journal of Materials Chemistry A*, 2013, **1**, 11543-11547.

49. M. Murase, N. Yabuuchi, Z.-J. Han, J.-Y. Son, Y.-T. Cui, H. Oji and S. Komaba, *ChemSusChem*, 2012, **5**, 2307-2311.

50. C. Kim, J. Y. Jang, N.-S. Choi and S. Park, *RSC Advances*, 2014, **4**, 3070-3074.

51. *Polymer Handbook*, John Wiley and Sons, New York, 1989.

52. *Lithium Ion Batteries: Science and Technology*, Springer Science + Business Media, LLC, 2009.

53. W.-R. Liu, M.-H. Yang, H.-C. Wu, S. M. Chiao and N.-L. Wu, *Electrochemical and Solid-State Letters*, 2005, **8**, A100-A103.

54. H. Buqa, M. Holzapfel, F. Krumeich, C. Veit and P. Novák, *Journal of Power Sources*, 2006, **161**, 617-622.

55. J. Li, R. B. Lewis and J. R. Dahn, *Electrochemical and Solid-State Letters*, 2007, **10**, A17-A20.

56. B. Key, R. Bhattacharyya, M. Morcrette, V. Seznéc, J.-M. Tarascon and C. P. Grey, *Journal of the American Chemical Society*, 2009, **131**, 9239-9249.

57. J. Guo and C. Wang, *Chemical Communications*, 2010, **46**, 1428-1430.

58. N. S. Hochgatterer, M. R. Schweiger, S. Koller, P. R. Raimann, T. Wöhrle, C. Wurm and M. Winter, *Electrochemical and Solid-State Letters*, 2008, **11**, A76-A80.

59. J. S. Bridel, T. Azaïs, M. Morcrette, J. M. Tarascon and D. Larcher, *Chemistry of Materials*, 2009, **22**, 1229-1241.

60. D. Mazouzi, B. Lestriez, L. Roué and D. Guyomard, *Electrochemical and Solid-State Letters*, 2009, **12**, A215-A218.

61. B. Lestriez, S. Bahri, I. Sandu, L. Roué and D. Guyomard, *Electrochemistry Communications*, 2007, **9**, 2801-2806.

62. L. El Ouatani, R. Dedryvère, J. B. Ledeuil, C. Siret, P. Biensan, J. Desbrières and D. Gonbeau, *Journal of Power Sources*, 2009, **189**, 72-80.

63. L. Yue, L. Zhang and H. Zhong, *Journal of Power Sources*, 2014, **247**, 327-331.

64. B. Koo, H. Kim, Y. Cho, K. T. Lee, N.-S. Choi and J. Cho, *Angewandte Chemie International Edition*, 2012, **51**, 8762-8767.
65. H. Lee, N. F. Scherer and P. B. Messersmith, *Proceedings of the National Academy of Sciences*, 2006, **103**, 12999-13003.
66. H. Lee, B. P. Lee and P. B. Messersmith, *Nature* 2007, **448**, 338-341.
67. M.-H. Ryou, J. Kim, I. Lee, S. Kim, Y. K. Jeong, S. Hong, J. H. Ryu, T.-S. Kim, J.-K. Park, H. Lee and J. W. Choi, *Advanced Materials*, 2013, **25**, 1571-1576.
68. Y. Park, S. Lee, S.-H. Kim, B. Y. Jang, J. S. Kim, S. M. Oh, J.-Y. Kim, N.-S. Choi, K. T. Lee and B.-S. Kim, *RSC Advances*, 2013, **3**, 12625-12630.
69. Y. K. Jeong, T.-w. Kwon, I. Lee, T.-S. Kim, A. Coskun and J. W. Choi, *Nano Letters*, 2014, **14**, 864-870.
70. J. L. Bredas and G. B. Street, *Accounts of Chemical Research*, 1985, **18**, 309-315.
71. G. Liu, S. Xun, N. Vukmirovic, X. Song, P. Olalde-Velasco, H. Zheng, V. S. Battaglia, L. Wang and W. Yang, *Advanced Materials*, 2011, **23**, 4679-4683.
72. J. Saint, M. Morcrette, D. Larcher, L. Laffont, S. Beattie, J. P. Pérès, D. Talaga, M. Couzi and J. M. Tarascon, *Advanced Functional Materials*, 2007, **17**, 1765-1774.
73. S. D. Beattie, D. Larcher, M. Morcrette, B. Simon and J.-M. Tarascon, *Journal of The Electrochemical Society*, 2008, **155**, A158-A163.
74. S. Xun, B. Xiang, A. Minor, V. Battaglia and G. Liu, *Journal of The Electrochemical Society*, 2013, **160**, A1380-A1383.
75. M. Wu, J. E. C. Sabisch, X. Song, A. M. Minor, V. S. Battaglia and G. Liu, *Nano Letters*, 2013, **13**, 5397-5402.
76. Z. Wang, Y. Fu, Z. Zhang, S. Yuan, K. Amine, V. Battaglia and G. Liu, *Journal of Power Sources*, 2014, **260**, 57-61.
77. J. T. Vaughey, G. Liu and J.-G. Zhang, *MRS Bulletin*, 2014, **39**, 429-435.
78. S. Xun, X. Song, V. Battaglia and G. Liu, *Journal of The Electrochemical Society*, 2013, **160**, A849-A855.
79. K. Dai, H. Zhao, Z. Wang, X. Song, V. Battaglia and G. Liu, *Journal of Power Sources*, 2014, **263**, 276-279.
80. M. Wu, X. Xiao, N. Vukmirovic, S. Xun, P. K. Das, X. Song, P. Olalde-Velasco, D. Wang, A. Z. Weber, L.-W. Wang, V. S. Battaglia, W. Yang and G. Liu, *Journal of the American Chemical Society*, 2013, **135**, 12048-12056.
81. B. Liu, P. Soares, C. Checkles, Y. Zhao and G. Yu, *Nano Letters*, 2013, **13**, 3414-3419.
82. M. Kummer, J. P. Badillo, A. Schmitz, H.-G. Bremes, M. Winter, C. Schulz and H. Wiggers, *J. Electrochem. Soc.*, 2014, **161**, A40-A45.
83. Z. Chen, J. W. F. To, C. Wang, Z. Lu, N. Liu, A. Chortos, L. Pan, F. Wei, Y. Cui and Z. Bao, *Advanced Energy Materials*, 2014, n/a-n/a.
84. U. Kasavajjula, C. Wang and A. J. Appleby, *Journal of Power Sources*, 2007, **163**, 1003-1039.
85. W.-R. Liu, Z.-Z. Guo, W.-S. Young, D.-T. Shieh, H.-C. Wu, M.-H. Yang and N.-L. Wu, *Journal of Power Sources*, 2005, **140**, 139-144.
86. B. C.-K. Tee, C. Wang, R. Allen and Z. Bao, *Nature Nanotechnology*, 2012, **7**, 825-832.
87. C. Wang, H. Wu, Z. Chen, M. T. McDowell, Y. Cui and Z. Bao, *Nature Chemistry*, 2013, **5**, 1042-1048.
88. C. K. Chan, H. Peng, G. Liu, K. McIlwrath, X. F. Zhang, R. A. Huggins and Y. Cui, *Nature Nanotechnology*, 2008, **3**, 31-35.
89. T. Yim, S. J. Choi, Y. N. Jo, T.-H. Kim, K. J. Kim, G. Jeong and Y.-J. Kim, *Electrochimica Acta*, **136**, 112-120.
90. B. Liu, A. Abouimrane, Y. Ren, M. Balasubramanian, D. Wang, Z. Z. Fang and K. Amine, *Chemistry of Materials*, 2012, **24**, 4653-4661.
91. L. Gong, M. H. T. Nguyen and E.-S. Oh, *Electrochem. Commun.*, 2013, **29**, 45-47.
92. H.-K. Park, B.-S. Kong and E.-S. Oh, *Electrochemistry Communications*, 2011, **13**, 1051-1053.
93. L. Yue, S. Wang, X. Zhao and L. Zhang, *Journal of Materials Chemistry*, 2012, **22**, 1094-1099.
94. Y. Chen, S. Zeng, J. Qian, Y. Wang, Y. Cao, H. Yang and X. Ai, *ACS Applied Materials & Interfaces*, 2014.
95. H. Zhao, X. Zhou, S.-J. Park, F. Shi, Y. Fu, M. Ling, N. Yuca, V. Battaglia and G. Liu, *Journal of Power Sources*, 2014, **263**, 288-295.

96.   H. Zhao, S.-J. Park, F. Shi, Y. Fu, V. Battaglia, P. N. Ross and G. Liu, *Journal of The Electrochemical Society*, 2014, **161**, A194-A200.
97.   S. S. Zhang, *Journal of Power Sources*, 2006, **162**, 1379-1394.
98.   V. Etacheri, O. Haik, Y. Goffer, G. A. Roberts, I. C. Stefan, R. Fasching and D. Aurbach, *Langmuir*, 2011, **28**, 965-976.
99.   M. Nie, D. P. Abraham, Y. Chen, A. Bose and B. L. Lucht, *The Journal of Physical Chemistry C*, 2013, **117**, 13403-13412.
100.   X. Chen, X. Li, D. Mei, J. Feng, M. Y. Hu, J. Hu, M. Engelhard, J. Zheng, W. Xu, J. Xiao, J. Liu and J.-G. Zhang, *ChemSusChem*, 2013, **7**, 549-554.
101.   J.-H. Kim, C.-M. Park, H. Kim, Y.-J. Kim and H.-J. Sohn, *Journal of Electroanalytical Chemistry*, 2011, **661**, 245-249.
102.   B. Guo, J. Shu, Z. Wang, H. Yang, L. Shi, Y. Liu and L. Chen, *Electrochemistry Communications*, 2008, **10**, 1876-1878.
103.   Y. Hwa, C.-M. Park and H.-J. Sohn, *Journal of Power Sources*, 2013, **222**, 129-134.
104.   B.-C. Yu, Y. Hwa, C.-M. Park and H.-J. Sohn, *Journal of Materials Chemistry A*, 2013, **1**, 4820-4825.
105.   W.-S. Chang, C.-M. Park, J.-H. Kim, Y.-U. Kim, G. Jeong and H.-J. Sohn, *Energy & Environmental Science*, 2012, **5**, 6895-6899.
106.   M. Yamada, A. Inaba, A. Ueda, K. Matsumoto, T. Iwasaki and T. Ohzuku, *Journal of The Electrochemical Society*, 2012, **159**, A1630-A1635.
107.   S. Xun, X. Song, M. E. Grass, D. K. Roseguo, Z. Liu, V. S. Battaglia and G. Liu, *Electrochemical and Solid-State Letters*, 2011, **14**, A61-A63.
108.   X. Huang, *Journal of Solid State Electrochemistry*, 2011, **15**, 649-662.
109.   L. Chen, X. Xie, J. Xie, K. Wang and J. Yang, *Journal of Applied Electrochemistry*, 2006, **36**, 1099-1104.
110.   J.-H. Lee, U. Paik, V. A. Hackley and Y.-M. Choi, *Journal of Power Sources*, 2006, **161**, 612-616.
111.   J. Chen, J. Liu, Y. Qi, T. Sun and X. Li, *Journal of The Electrochemical Society*, 2013, **160**, A1502-A1509.
112.   M. N. Obrovac, L. Christensen, D. B. Le and J. R. Dahn, *Journal of The Electrochemical Society*, 2007, **154**, A849-A855.
113.   N. Liu, Z. Lu, J. Zhao, M. T. McDowell, H.-W. Lee, W. Zhao and Y. Cui, *Nature Nanotechnology*, 2014, **9**, 187-192.
114.   Z. Du, R. A. Dunlap and M. N. Obrovac, *Journal of the Electrochemical Society*, 2014, **161**.

TOC figure

A conductive polymer binder is in-situ doped, enabling a long-term cycling stability of silicon.

A mussel inspired polymer binder improves adhesion.

A 3-dimentional porous conductive polymer framework is in-situ generated to encapsulate silicon nanoparticles.

2011   **2012**   **2013**   **2014**

Carboxymethyl cellulose (CMC) was established as an effective binder for a silicon anode. Hydrogen bonding between the polymer backbone and silicon oxide surface layer plays an important role.

Alginate, a natural polysaccharide extracted from brown algae, yields a stable battery anode when mixed with Si nanopowder.

A multifunctional binder maintains electronic conductivity, adhesion, ductility, and electrolyte Uptake.

A self-healing polymer repairs damage and cracks.

Hui Zhao has been a chemist postdoctoral fellow in Dr. Gao Liu's group at Lawrence Berkeley

National Laboratory since 2013. Hui earned his Ph.D. degree in Organic and Polymer Chemistry from Michigan State University in 2012, with a focus on the chemical synthesis and electrochemical performance of polyethylene glycol-based single lithium-ion conductors. His current interests include novel electrolytes and polymer binders for silicon anodes in lithium-ion batteries.

Wen Yuan received a B.S. in Chemistry from Nanjing University in 2008 and a Ph.D in Polymer/Organic Chemistry from Michigan State University in 2013. He is currently working as a chemist postdoc fellow at Lawrence Berkeley National Lab. His research interest includes applications of novel polymer materials for energy storage and conversion.

Dr. Gao Liu received B.S. in Applied Chemistry from Beijing University in 1993 and Ph.D. in Chemistry from Michigan State University in 2001. After that, he worked as a Post-doctoral Fellow in the Electrochemistry Group at Lawrence Berkeley National Laboratory. He currently serves as a Staff Scientist and Principal Investigator under U.S. Department of Energy (DOE) Battery for Advanced

Transportation Technologies Program (BATT), Applied Batteries Research Program (ABR) and for industry sponsored program at Lawrence Berkeley National Laboratory. His current research combines synthetic polymer chemistry, composite engineering, and electrochemistry to solve the interdisciplinary problems in energy generation, storage, and usage.